ORIGINAL PAPER

Effect of Nb alloying additions on the characteristics of anodic oxide films on zirconium and their stability in NaOH solution

**Francesco Rosalbino · Daniele Macciò ·
Adriana Saccone · Emma Angelini · Stefano Delfino**

Abstract The characteristics of oxide films on Zr and Zr–Nb alloys (with Nb content of 2.5, 5, and 10 at.%) galvanostatically formed (at a current density of 100 μA cm^{-2}) in 0.5 M H$_2$SO$_4$ solution were investigated by means of electrochemical impedance spectroscopy. Electrochemical impedance spectroscopy spectra were interpreted in terms of an "equivalent circuit" with the circuit elements representing the electrochemical properties of a single layer oxide. The resistance of the oxide films was found to increase with increased Nb content in the alloy while the capacitance showed an opposite trend. The stability of the anodic oxide films grown in the sulfuric acid solution on Zr and Zr–Nb alloys was investigated by simultaneously measuring the electrode capacitance and resistance at a working frequency of 1 kHz as a function of exposure time to naturally aerated 3 M NaOH solution. Analyses of the electrode capacitance and resistance values indicated a decrease in chemical dissolution rate of the oxide films with the increase of Nb content in the alloy.
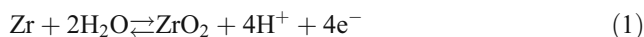
F. Rosalbino (✉) · E. Angelini
Politecnico di Torino, Dipartimento di Scienza dei Materiali e
Ingegneria Chimica (DICHI),
Corso Duca degli Abruzzi 24,
10129 Torino, Italy
e-mail: francesco.rosalbino@polito.it

D. Macciò · A. Saccone · S. Delfino
Università degli Studi di Genova,
Dipartimento di Chimica e Chimica Industriale (DCCI),
Via Dodecaneso 31,
16146 Genova, Italy

Introduction

Zirconium (Zr) has been the subject of numerous investigations, mainly because of the stability of its passive film toward corrosion and hydrogen embrittlement and its small cross section for neutron absorption, which makes it a suitable material for use as pressure tubes immersed in lithiated heavy water for nuclear fuels [1]. Moreover, the great demand of stable materials to be used in thermal reactors, chemical industries, and electrochemical methods of the PUREX process for waste minimization [2, 3] makes the corrosion and passivation of zirconium and its alloys important cases worthy of intensive studies.

The electrochemical stability of zirconium, a valve metal, is attributed to the stability and thickness of the ZrO$_2$ film covering the unstable bare metal [4]. In aqueous solutions, the standard potential at 25 °C for reaction 1 is −1.46 V/RHE:

$$Zr + 2H_2O \rightleftarrows ZrO_2 + 4H^+ + 4e^- \qquad (1)$$

Thus, the bare metal is always covered by a very thin oxide layer. Such a film is responsible for the apparent behavior of the metal under open circuit conditions or under the influence of an alternating field, since the film acts as a source or sink for electrons which participate in the electrochemical reaction.

Like zirconium, niobium (Nb) forms passive films in a wide variety of media and can be covered with a stable oxide film (Nb$_2$O$_5$) protecting it from continuous corrosion [5]. Nevertheless, Nb is more corrosion resistant than Zr due to the higher stability of its oxide, and Zr–Nb alloys were developed in order to improve the corrosion resistance of Zr [6–8]. The enhanced corrosion behavior of Nb-containing Zr alloys in aqueous solutions has been ascribed to the passive film formed on their surface [6–8]. Thus,

characterization of the passive films is essential for the understanding of the corrosion behavior of these alloys in aqueous environments.

Very few papers are concerned with the electrochemical behavior of anodic oxide films on zirconium in alkaline solutions using electrochemical methods, and no data were found on Zr–Nb alloys. It was shown that the oxide films on zirconium anodically formed in 0.5 M H_2SO_4 solution are fairly stable in alkali concentration ≤1 M, while they are highly unstable when immersed in more concentrated solutions [9, 10].

The aim of the present work is to examine the effect of Nb alloying additions (up to 10 at.%) on the characteristics of anodically formed oxide films on Zr and their stability in NaOH solution of concentration >1 M. This was done using galvanostatic and electrochemical impedance spectroscopy (EIS) techniques.

Experimental

The metals used were Zr (99.8 mass%, NewMet Koch, Waltham Abbey, UK) and Nb (99.6 mass%, H.C. Starck, Inc., Newton, MA, USA). The Zr–Nb alloys (with Nb contents of 2.5, 5, and 10 at.%), having a mass of about 2 g each, were prepared by arc melting starting from pieces of metals in inert Ar atmosphere. The samples were melted and reversed at least five times to assure homogeneity. These alloys were characterized using energy-dispersive X-ray analysis (EDX), scanning electron microscopy (SEM), and X-ray diffraction (XRD); a detailed description of the alloys' microstructure was reported elsewhere [11].

The Zr–Nb samples were made into electrodes by inserting insulated copper wires and protecting all sides but one with epoxy resin. The exposed surface area was 0.25 cm^2. Before each experiment, the electrode surface was mechanically polished using successively finer grades of emery paper until a mirror-bright surface was attained. The electrode was then immediately immersed in 0.5 M H_2SO_4 solution, previously purged of oxygen by purified nitrogen. A large platinum sheet served as counter electrode, and all potentials measurements were made with reference to a saturated calomel electrode. Electrochemical measurements were performed using a Solartron 1286 Electrochemical Interface controlled by a computer. Oxide films on Zr and Zr–Nb alloys were formed under conditions of galvanostatic anodizing. During anodizing, the anodic charging curves were recorded at a current density of 100 μA cm^{-2} for a period of 5 min. After anodizing, the oxide film was stabilized at the open circuit potential (E_{OCP}) for a period of 30 min, after which, impedance measurements were performed. EIS was used to determine

the characteristic magnitudes of the oxide films anodically formed on Zr and Zr–Nb alloys. Impedance spectra were recorded at E_{OCP} using an EG&G PAR system Model 2263 driven by a computer. The frequency studied ranged from 100 kHz to 10 mHz at seven points per decade. The amplitude of the sinusoidal perturbation signal was 10 mV. Data were stored in the computer and processed according to the EQUIVCRT program (B.A. Boukamp, University of Twente).

The stability of the anodic oxides obtained in sulfuric acid solution on Zr and Zr–Nb alloys was investigated by simultaneously measuring the electrode capacitance, C_m, and resistance, R_m, (working frequency=1 kHz, amplitude of the sinusoidal perturbation signal=10 mV) in naturally aerated 3 M NaOH solution at 25 °C as a function of exposure time.

Results and discussion

The EDX analysis confirmed the nominal composition of the samples. SEM characterization reveals that all the alloys are single-phase, laying in the continuous solid solution (βZr,Nb) field. XRD patterns match with these results, as they show a cI2-W type structure stable at high temperature (solid solution (βZr,Nb)) [11].

Figure 1 shows the anodic charging curves for Zr and Zr–Nb alloys in 0.5 M H_2SO_4 solution at the current density of 100 μA cm^{-2}. A linear increase of potential with time is observed in all cases. During formation of the oxide layer at the constant current density, each newly formed part of the oxide layer, dd, requires an increase in voltage, dE, in order for the electric field within the oxide, and thereby the current of anodizing, to remain constant. If the voltage drop on the already formed oxide layer does not change during anodizing, the value dE/dd will be deter-
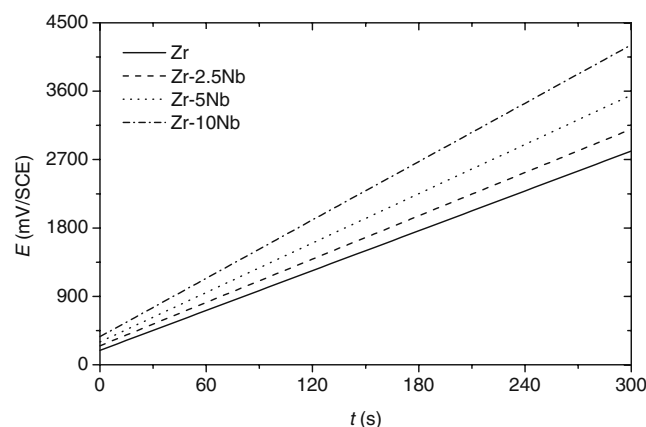

Fig. 1 Anodic charging curves of Zr and Zr–Nb alloys in 0.5 M H_2SO_4 solution at a current density of 100 μA cm^{-2}

mined precisely by the increasing part of the layer. Therefore, the rate of potential increase with time represents the rate of oxide formation, dE/dt [12]. As can be seen in Fig. 2, the oxide formation rate, dE/dt, increases with the increase of Nb content in the alloy. A higher slope of the anodic charging curves is related to a more resistant character of the oxide film, which could be ascribed to a greater thickness or to a more insulating character. Ellipsometric characterizations are being carried out in order to evaluate the thickness of the anodic oxide films on Zr–Nb alloys. A similar behavior was observed by Gudić et al. for anodic oxide films anodically grown at 100 μA cm^{-2} on Al–Sn and Al–In alloys [13, 14].

The characteristic magnitudes of oxide films were determined by measurement of impedance of Zr(Zr–Nb alloy)/oxide film/electrolyte systems. Anodic oxide films were formed galvanostatically on Zr and Zr–Nb electrodes in 0.5 M H$_2$SO$_4$ solution at the current density of 100 μA cm^{-2}. After anodizing for 5 min and reaching a certain potential, the current was switched off, and the impedance measurements were performed at the open circuit potential, E_{OCP}, after stabilization at E_{OCP} for 30 min. Impedance spectra for Zr and Zr–Nb alloys are presented as Nyquist plots in Fig. 3. The response of the system in the Nyquist complex plane was a single capacitive arc that can be correlated with the dielectric properties of the oxide film. As can be seen in Fig. 3, the diameter of the capacitive arc increases with increasing Nb content in the alloy. A satisfactory fitting of all data could be obtained using a simple $R_s(QR_p)$ circuit (Fig. 4), where R_s and R_p are the solution and the parallel (oxide film) resistances, respectively, and Q is a constant phase element (CPE), which takes into account the capacitive behavior of the film. Oliveira et al. [15, 16] proposed $R_s(QR_p)$ as the equivalent circuit model to fit the EIS data in the case of a single passive film anodically grown on Ti–Zr and Ti–Nb alloys in 0.5 M H$_2$SO$_4$ solution. The
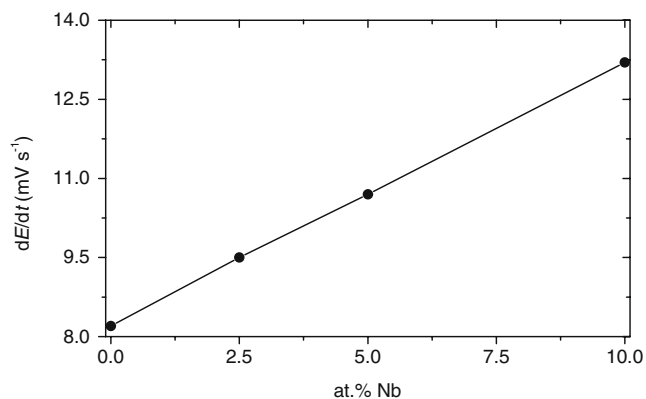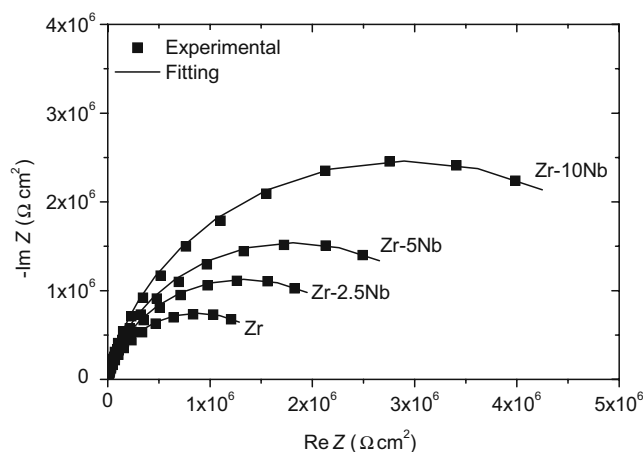

Fig. 3 Nyquist plots for the impedance of the galvanostatically formed oxide films on Zr and Zr–Nb alloys at 100 μA cm^{-2} in 0.5 M H$_2$SO$_4$ solution obtained after stabilization at the open circuit potential for 30 min

impedance, Z_{CPE}, of CPE is described by the expression [17–19]:

$$Z_{CPE} = [Q(j\omega)^n]^{-1}$$

with $-1 \leq n \leq 1$ and $j = \sqrt{-1}$, while Q is a frequency-independent constant, being defined as pure capacitance for $n=1$, resistance for $n=0$, inductance for $n=-1$. Diffusion processes are characterized by the value of $n=0.5$. According to the fitting results, the n values are >0.9 indicating that $Q \approx C$.

The parameters of the equivalent circuit R_s, R_p, and Q are presented in Table 1. As can be seen, when the Nb content in the alloy increases, the value of the oxide resistance increases and the value of the capacitance decreases, which indicates an increase of the insulating character of the oxide film. As a consequence, anodically formed oxide films are expected to display better corrosion resistance with higher Nb content in the alloy, as already observed by Gudić et al. for Al–Sn and Al–In alloys [13, 14].

In order to confirm this hypothesis, electrode capacitance, C_m, and resistance, R_m, were simultaneously measured in 3 M NaOH solution where anodic oxide films on pure Zr are highly unstable [9, 10]. The oxide films were formed by galvanostatic anodizing at a current density of 100 μA cm^{-2} for a period of 5 min in 0.5 M H$_2$SO$_4$ solution. After a 30-min stabilization at the open circuit

Fig. 2 Dependence of oxide formation rate on Nb content in the alloy

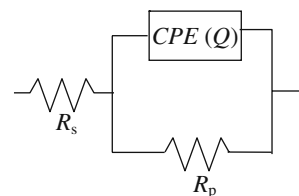**Fig. 4** Equivalent circuit, $R_s(QR_p)$, used to fit the experimental impedance data

Table 1 Electrical parameters of equivalent circuit obtained by fitting the experimental results of EIS

Sample	R_s ($\Omega\,cm^2$)	Q ($\mu\,cm^{-2}\,s^{n-1}$)	n values	R_p ($M\Omega\,cm^2$)
Zr	1.52	9.52	0.93	1.62
Zr–2.5Nb	1.53	8.21	0.94	2.44
Zr–5Nb	1.54	6.53	0.95	3.57
Zr–10Nb	1.56	4.35	0.97	5.79

potential, the electrode was rinsed with triply distilled water and transferred immediately to the electrochemical cell containing the dissolution medium where the electrode capacitance, C_m, and resistance, R_m, were traced with time for about 6 h. The variation of the resistance, R_m, and the reciprocal capacitance, C_m^{-1}, with time in naturally aerated 3 M NaOH solution is illustrated in Fig. 5. A rapid decrease in R_m and C_m^{-1} followed by a slow decay to attain a steady state value is observed in all cases. The same trend was already observed both in NaOH solutions of concentration >1 M and in 0.05 M HF solution for anodically formed oxide films on Zr [9, 10, 20]. The drift of R_m and C_m^{-1} to lower values with time indicates that the anodic oxide films are subjected to a chemical dissolution process activated by OH⁻ ions [9, 10]. However, the steady state values of R_m and C_m^{-1} increase with increasing Nb content in the alloy, as inferred from Fig. 5, indicating a decrease in the chemical dissolution rate of the oxide film [9, 10, 20].

During anodic oxidation of Zr–Nb alloys, niobium species may be incorporated into the oxide film. Nb is a strong oxide former [21], resists to chemical dissolution in high pH environments [22, 23], and easily forms M–O bonds of high strength [21]. Yu et al. [24, 25] investigated the effects of Nb and Zr alloying additions on the activation of Ti and suggested the formation of mixed Ti–Zr or Ti–Nb oxides that are thermodynamically stable and protected from active dissolution of Ti. Moreover, Olivera et al. [15, 16], using X-ray photoelectron spectroscopy (XPS) studies, claimed that films anodically grown on Ti–Zr and Ti–Nb alloys in 0.5 M H_2SO_4 solution consist of a single layer mixed oxide phase containing both TiO_2 and ZrO_2 or TiO_2 and Nb_2O_5 groups.

There are very few studies on the passive behavior of Zr–Nb alloys in the literature. The only available experimental results confirming the presence of niobium in the oxide film on Zr–Nb alloys have been published by Kim and coworkers [26]. Using the photo-electrochemical analysis, these authors claimed that the anodically formed oxide films of on Zr–Nb alloys with niobium contents up to 2.5 at.% consist of a single layer containing a mixture of zirconium oxide and niobium oxide.

Data reported in the present study show: (a) the presence of niobium in the alloy improves the oxide film dielectric properties (increased resistance and decreased capacitance) and (b) the presence of niobium increases the resistance of the oxide film to chemical dissolution. Thence, the results obtained lead to the conclusion that the presence of increasing oxidized Nb amounts in the passive layer can progressively reduce surface activation in alkaline solution, thereby improving the stability and, therefore, the chemical dissolution resistance of the anodically formed oxide films on Zr–Nb alloys. On the other hand, similar results were found on Ti–Nb alloys in chloride-containing solutions [27].

Conclusions

The characteristics of oxide films on Zr and Zr–Nb alloys (with Nb content of 2.5, 5, and 10 at.%) galvanostatically formed in 0.5 M H_2SO_4 solution were investigated by means of electrochemical impedance spectroscopy.
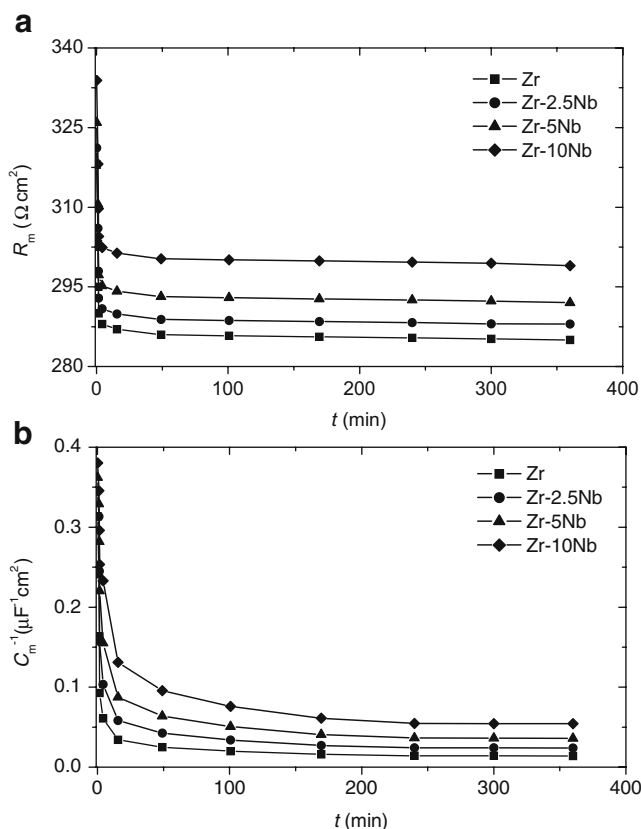

Fig. 5 a Resistance, R_m, and **b** reciprocal capacitance, C_m^{-1}, of anodized Zr and Zr–Nb alloys as a function of exposure time to naturally aerated 3 M NaOH solution

Anodic charging curves recorded at a current density of $100~\mu A~cm^{-2}$ highlighted an increase of the oxide formation rate with the increase of Nb content in the alloy.

EIS results indicated that the films grown on Zr and Zr–Nb alloys are composed of a single layer oxide whose resistance increases with increasing Nb amount in the alloy while the capacitance shows an opposite trend.

The electrode capacitance and resistance measurements carried out in naturally aerated 3 M NaOH solution showed the beneficial effect of increasing Nb contents in the alloy on the oxide films stability.

References

1. Franklin DG, Lang PM, Garde AM (1991) Proceeding of the 9th international symposium on zirconium in the nuclear industry. ASTM, Philadelphia
2. Chatainier G, Petit JA, Dabosi F (1978) Corros Sci 18:961
3. Marx G, Bestanpouri A, Droste R, Erben W, Schonemann W, Wagen D (1986) J Less Common Metals 121:507
4. Bard AJ (1986) Encyclopedia of electrochemistry of the elements. Marcel Dekker, New York
5. Yau TL, Webster R (1993) ASM Handbook, Corrosion, vol 13. ASM International, Metals Park
6. Olsson C-OA, Landolt D (2003) Electrochim Acta 48:3999
7. Arima T, Miyata K, Inagaki Y, Idemitsu K (2005) Corros Sci 47:435
8. Kim HG, Park SY, Lee MH, Jeong YH, Kim SD (2008) J Nucl Mater 373:429
9. Gad Allah AG, Abd El-Rahman HA, Abou-Romia MM (1988) J Appl Electrochem 18:532
10. Gad Allah AG, Mazhar AA, El-Taib Heakal F, Ameer MA (1989) J Appl Electrochem 19:213
11. Rosalbino F, Macciò D, Saccone A, Angelini E, Delfino S (2009) Corros Sci (in press)
12. Gudić S, Radošević J, Krpan-Lisica D, Kliškić M (2001) Electrochim Acta 46:2515
13. Gudić S, Radošević J, Kliškić M (2002) Electrochim Acta 47:3009
14. Gudić S, Radošević J, Višekruna A, Kliškić M (2004) Electrochim Acta 49:773
15. Oliveira NTC, Biaggio SR, Piazza S, Sunseri C, Di Quarto F (2004) Electrochim Acta 49:4563
16. Oliveira NTC, Biaggio SR, Nascente PAP, Piazza S, Sunseri C, Di Quarto F (2006) Electrochim Acta 51:3506
17. Macdonald JR (1987) Impedance spectroscopy. Wiley, New York
18. Rammelt U, Reinhard G (1990) Electrochim Acta 35:1045
19. Stoyanov Z (1990) Electrochim Acta 35:1493
20. Huot J-Y (1992) J Appl Electrochem 22:852
21. Marcus P (1994) Corros Sci 36:2155
22. Corvino BS, Carter JP, Cramer SD (1980) Corrosion 36:554
23. Hurlen T, Bentzen H, Hornkjøl S (1987) Electrochim Acta 32:1613
24. Yu SY, Brodrick CW, Ryan MP, Scully JR (1999) J Electrochem Soc 46:4429
25. Yu SY, Scully JR, Vitus CM (2001) J Electrochem Soc 148:B68
26. Kim B-Y, Park C-J, Kwon H-S (2005) J Electroanal Chem 576:269
27. Yu SY, Scully JR (1997) Corrosion 53:468